

## Chapter 23

# Other Main Sequences

The simplicity and the importance of the results obtained for the main sequence suggest the extension of this concept to stars of quite different composition. We can then describe a main sequence as any sequence of homogeneous models with various masses  $M$  in complete equilibrium, consisting (mainly) of a certain element which burns in the central region. In this sense, *the* (normal) main sequence as treated before is a special case and is more precisely called the *hydrogen main sequence* (H-MS). In a further step of generalization, we will even drop the assumption of chemical homogeneity, thus arriving at the so-called generalized main sequences (GMS) (Sect. 23.3). Of course, compared with the H-MS, the other sequences are far less important for real, observed stars. But their properties yield valuable information for understanding certain types of evolved stars, for example.

The numerical models shown in this chapter have been calculated with an older equation of state and simpler opacities. Also, the chemical composition for the hydrogen-rich models differs from that used in the last chapter and is for a slightly higher (= 0.021) metallicity. But since we will discuss fundamental properties of stars in this section, these details are of no relevance.

### 23.1 The Helium Main Sequence

The helium main sequence (He-MS) contains chemically homogeneous equilibrium models that consist almost completely of He (with the usual few per cent of heavier elements) and have central helium burning. In principle, one could imagine them to be the descendants of perfectly mixed hydrogen-burning stars (however, perfect mixing during evolution is very improbable). Or they may represent the remnants of originally more massive stars that have developed a central helium core and then lost their hydrogen-rich envelope.

In the Hertzsprung–Russell diagram (Fig. 23.1) the He-MS is situated far to the left of the (normal) H-MS at fairly high luminosities. If we compare the same stellar

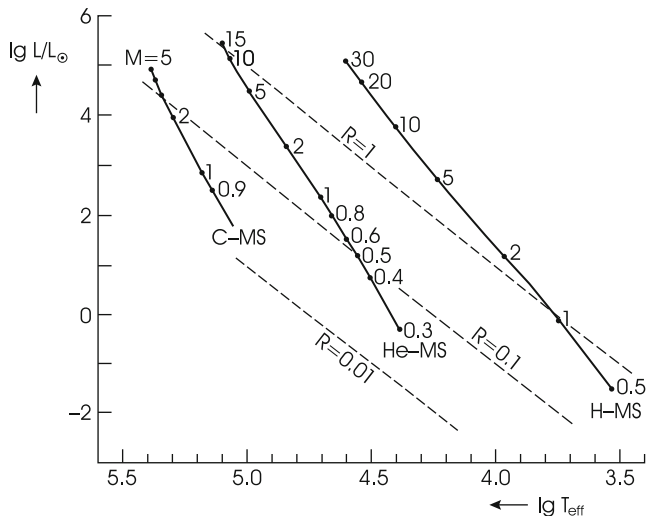


**Fig. 23.1** In the Hertzsprung–Russell diagram the *solid lines* show the normal hydrogen main sequence (H-MS;  $X_{\text{H}} = 0.685$ ,  $X_{\text{He}} = 0.294$ ), the helium main sequence (He-MS;  $X_{\text{H}} = 0$ ,  $X_{\text{He}} = 0.979$ ), and the carbon main sequence (C-MS;  $X_{\text{H}} = X_{\text{He}} = 0$ ,  $X_{\text{C}} = X_{\text{O}} = 0.497$ ). The *labels* along the sequences give stellar masses  $M$  (in units of  $M_{\odot}$ ). Three lines of constant stellar radius ( $R$  in units of  $R_{\odot}$ ) are plotted (*dashed*)

mass  $M$  on each sequence, we see that the helium stars have smaller radii and much higher luminosities. The remarkable difference in  $L$  for given  $M$  is particularly well illustrated by the  $M - L$  relations in Fig. 23.2. The main cause is certainly the difference in the mean molecular weight  $\mu$ , which is 0.624 for the mixture used for the stars on the H-MS and 1.343 for the helium stars. If everything else were the same and the models were homologous, then we would expect from (20.20) for stars with the same  $M$  a difference in luminosity given by  $\Delta \lg L = 4\Delta \lg \mu = 1.33$ . This is in fact very nearly the shift between the two  $M - L$  relations in Fig. 23.2 at  $M = 10M_{\odot}$ , while for  $M = 1M_{\odot}$ , we even have  $\Delta \lg L \approx 2.5$ .

The interior structure resembles roughly that of models on the upper H-MS. The extreme temperature sensitivity of helium burning concentrates the energy production into a small central sphere where the large energy flux produces a convective core. This contains about  $0.27M$  in the  $1M_{\odot}$  star, and nearly  $0.7M$  for  $10M_{\odot}$ . The increase of the convective core is again a consequence of the increasing radiation pressure: it contributes 1.5% to the total pressure in the centre of the  $1M_{\odot}$  star, 18% for  $5M_{\odot}$ , and 32% for  $10M_{\odot}$ , which is very much more than for the corresponding stars on the H-MS ( $6 \times 10^{-4}$ , 0.018, and 0.063, respectively). The difference is due to the fact that helium burning requires temperatures roughly six times higher, as can be seen in Fig. 23.3, which shows the central values of  $T$  and  $\rho$ . The high radiation pressure provides relatively large amplitudes of pulsation in the central region. This again produces a vibrational instability due to the  $\epsilon$  mechanism,

**Fig. 23.2** Mass–luminosity relations for the models of the hydrogen, helium, and carbon main sequences of Fig. 23.1

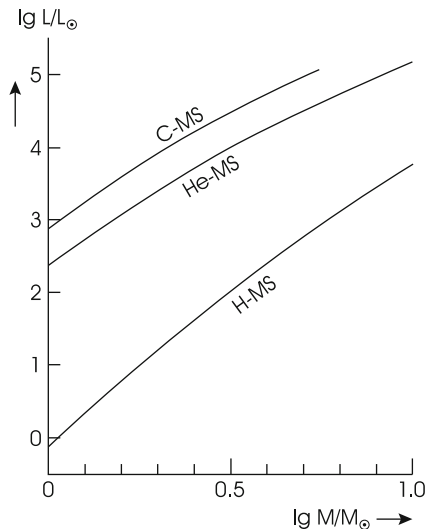
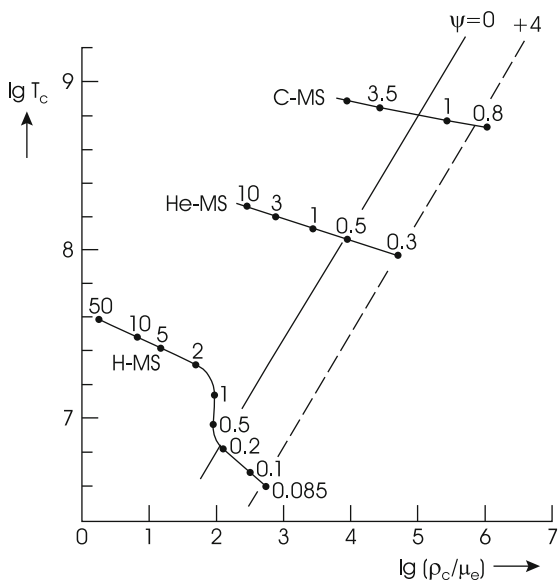


**Fig. 23.3** Central temperature  $T_c$  (in K) and central density  $\rho_c/\mu_e$  ( $\rho_c$  in  $\text{g cm}^{-3}$ ,  $\mu_e$  = molecular weight per electron) of the models on the hydrogen, helium, and carbon main sequences of Fig. 23.1. The labels along the lines give the stellar mass  $M$  (in  $M_{\odot}$ ). The dashed lines indicate constant degeneracy parameters  $\psi$  of the electron gas



the onset of which occurs around  $M = 15M_{\odot}$ , depending somewhat on the content of heavier elements.

Another property of the helium stars to be seen in Fig. 23.3 is their much larger central density: for  $M = 0.3M_{\odot}$ ,  $\rho_c$  reaches  $10^5 \text{ g cm}^{-3}$ , and, in spite of the larger  $T$ , the electron gas has about the same degree of degeneracy as at the lower end of the H-MS [In order to plot a unique degeneracy parameter  $\psi$  (see Chap. 15) for compositions with different molecular weight per electron  $\mu_e$ , the abscissa of

Fig. 23.3 gives  $\lg(\rho_c/\mu_e)$ . The He-MS and the C-MS (see below) have  $\mu_e = 2$ , while  $\mu_e = 1.19$  for the plotted H-MS.]. The increasing degeneracy causes the sequence of stable helium-burning stars to terminate at about  $M \approx 0.3M_\odot$ .

## 23.2 The Carbon Main Sequence

The next major step in the nuclear history of a star is carbon burning. Thus, we now consider a carbon main sequence (C-MS) consisting of homogeneous models in complete equilibrium that have central carbon burning. Except for the usual admixture of a few per cent of heavy elements, the composition can be either pure  $^{12}\text{C}$ , or a mixture of  $^{12}\text{C}$  and  $^{16}\text{O}$  in equal amounts, which represents roughly the end products of stellar helium burning (For both assumptions the basic results, in particular the luminosities, are not too different, since the molecular weights are nearly the same.). The models of the C-MS are not so much used for describing homogeneous carbon stars, but rather for the purpose of surveying carbon-burning cores in highly evolved stars.

In the Hertzsprung–Russell diagram (Fig. 23.1) the C-MS is at  $T_{\text{eff}} > 10^5$  K even to the left of the He-MS. For equal masses, models on the C-MS have remarkably smaller  $R$  and larger  $L$ . The  $M - L$  relation for carbon stars is  $\Delta \lg L \approx 0.5$  above that for helium stars (Fig. 23.2) because of the larger mean molecular weight ( $\Delta \lg \mu \approx 0.11$ ).

The interior solutions of carbon stars have similar properties to those of the helium stars, for example, large convective cores and an appreciable amount of radiation pressure. In a model of  $M = 3.5M_\odot$ , the convective core encompasses about 45% of the total mass, and the radiation pressure contributes more than 20% to the central pressure. Figure 23.3 shows that, according to the requirements of carbon burning, the central temperatures are between  $5$  and  $8 \times 10^8$  K. But the central density is even more increased compared to helium stars. Therefore appreciable degeneracy of the electron gas is already found in carbon stars around  $1M_\odot$ . And the sequence of stars with a stable carbon burning terminates at masses in the range  $M \approx 0.9 \dots 0.8M_\odot$ . The exact value of this limiting mass depends somewhat on the assumptions in the physical parameters. A well-known uncertainty comes, for example, from neutrino losses, which can become noticeable in these very hot and dense stars (Sect. 18.7). Large neutrino losses have the tendency to increase the lower limit of  $M$  for stable carbon burning. Figure 23.3 shows that in all three main sequences the limiting mass occurs at roughly the same degree of degeneracy of the electron gas ( $\psi \approx 4.5$ ). The C-MS and the He-MS have a much simpler structure than the H-MS, which is affected by the complications occurring near  $1M_\odot$ , namely the transition from convective to radiative cores and the growth of outer convection zones with decreasing  $T_{\text{eff}}$ .

## 23.3 Generalized Main Sequences

The logical next step in extending the concept of main sequences is to drop the condition of chemical homogeneity. This is suggested by the chemical evolution we encounter in all stars: the conversion of hydrogen to helium by nuclear reactions (which are concentrated towards the centre) produces a central helium core, while the outer envelope retains its original hydrogen-rich mixture. If the temperatures are high enough, helium burning will occur around the centre, and hydrogen burning continues in a so-called shell source, i.e. a concentric shell starting at the bottom of the hydrogen-rich envelope. Based on this picture, different types of significant sequences may be defined. We will limit ourselves in the following to the simplest case, which nevertheless finds useful applications.

For these *generalized main sequences* (GMS), we consider models in complete equilibrium, with a chemical profile as shown in Fig. 23.4: a central helium core of mass  $M_{\text{He}}$ , i.e. of the mass fraction  $q_0 = M_{\text{He}}/M$ , is surrounded by an envelope of mass  $(1 - q_0)M$  with the usual hydrogen-rich mixture of unevolved stars. At the interface of the two regions, the hydrogen content  $X_{\text{H}}$  changes discontinuously (“step profile”), while the hydrogen content in the envelope as well as the small admixture of heavier elements in both regions is assumed to be fixed at some reasonable values. The energy is supplied by central helium burning and (possibly) by an additional hydrogen burning in a shell source at  $q_0$ .

Each of these models is characterized by two parameters, the stellar mass  $M$ , and the relative core mass  $q_0$ . We then obtain a generalized main sequence by keeping  $q_0$  constant and varying  $M$  as a parameter. For each value of  $q_0$  there is one GMS. In the evolution the value of  $q_0$  is not constant:  $q_0$  can slowly increase because of the shell source burning, and it can increase by mass loss from the surface. We will therefore consider GMS of various values of  $q_0$ .

The upper limit is obviously  $q_0 = 1$ , implying that the “core” encompasses the whole star, which is then a homogeneous helium star. The GMS for  $q_0 = 1$  is therefore identical with the well-known He-MS discussed in Sect. 23.1.

For values of  $q_0$  slightly below 1, the GMS are shifted appreciably to the right in the Hertzsprung–Russell diagram (Fig. 23.5). They have already passed the H-MS for  $q_0 \approx 0.9 \dots 0.85$ , depending on the value of  $M$ . In other words, the addition of a relatively small hydrogen-rich layer on top of a helium star will remarkably increase its radius and decrease  $T_{\text{eff}}$ .

This behaviour changes completely if  $q_0$  drops below a certain value, which is about  $0.8 \dots 0.7$ , depending on  $M$ . Figure 23.5 shows that the GMS are then compressed towards a limiting line far to the right-hand side of the Hertzsprung–Russell diagram. This will turn out to be the Hayashi line, a limit for all stars in hydrostatic equilibrium (Chap. 24). The closest approach to it is found roughly for the GMS with  $q_0 = 0.5$ . For even smaller  $q_0$ , the GMS move slowly back to the left in the Hertzsprung–Russell diagram. We conclude that the upper part of this diagram can be covered at least once by these GMS, i.e. by very simple equilibrium models depending on two parameters ( $M, q_0$ ) only.

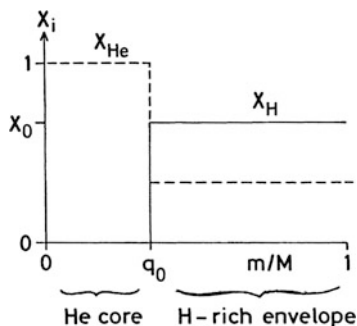


**Fig. 23.4** Chemical composition inside the models on the generalized main sequences. The mass concentrations of hydrogen  $X_H$  (solid line) and helium  $X_{He}$  (dashed line) are plotted over the mass variable  $m/M$  from centre to surface.  $X_0$  is the hydrogen content in the envelope. The relative core mass is  $M_{He}/M = q_0$

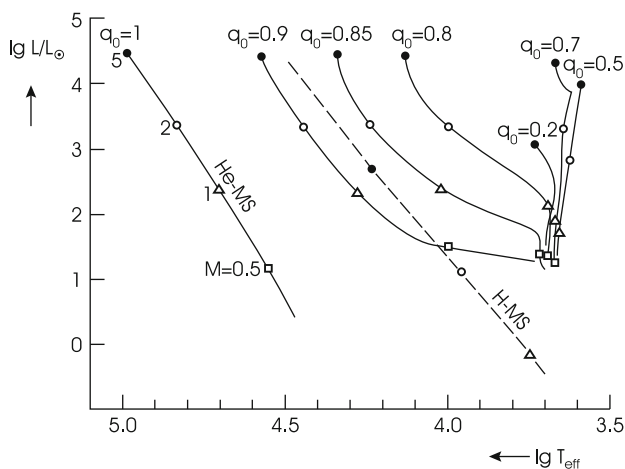


**Fig. 23.5** Hertzsprung–Russell diagram with generalized main sequences for models with helium cores of relative mass  $q_0$  and hydrogen-rich envelopes of relative mass  $1 - q_0$  (cf. Fig. 23.4). The sequences plotted here cover only the range from  $q_0 = 1$  (helium main sequence) to  $q_0 = 0.2$ . For comparison, the limiting case of the hydrogen main sequence ( $q_0 = 0$ , dashed) is shown. Models with a stellar mass  $M = 5$  (in  $M_\odot$ ) are indicated by solid dots,  $M = 2$  by open circles,  $M = 1$  by triangles, and  $M = 0.5$  by squares (After Giannone et al. 1968)

Let us compare models with the same  $M$  on different GMS. If we connect their points in Fig. 23.5, we obtain curves such as those plotted in Fig. 23.6 for two values of  $M$ . This shows that the luminosity remains roughly constant in the range  $q_0 = 1 \dots 0.7$ . This is caused by two opposite effects nearly cancelling each other: when we decrease  $q_0$  at  $M = \text{constant}$ ,  $M_{He}$  decreases, which reduces the luminosity of the core,  $L_{He}$ , approximately as given by the  $M - L$  relation for the He-MS (Fig. 23.2, if here we take  $M_{He}$  for  $M$ ). At the same rate, the mass of the

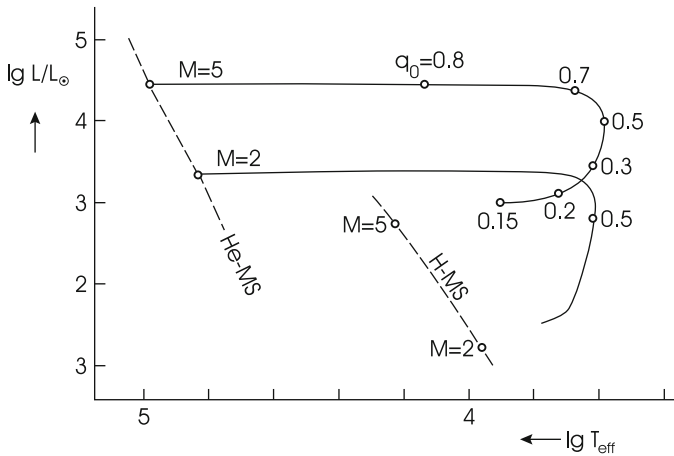


**Fig. 23.6** The solid lines connect models of the same stellar mass  $M$  (in  $M_{\odot}$ ) on the different generalized main sequences of Fig. 23.5. Labels along the lines give the  $q_0$  values of the generalized main sequences (After Lauterborn, Refsdal, Weigert, 1971a)

envelope  $M(1 - q_0)$  increases, which gives an increasing energy production  $L_H$  of the hydrogen shell source, such that the total luminosity  $L = L_{\text{He}} + L_H$  can remain almost constant. The situation changes when  $q_0$  drops below, say, 0.7. The “helium luminosity”  $L_{\text{He}}$  then decreases so strongly that it is compensated no longer by the increase of  $L_H$ , which eventually dominates  $L$  completely.

Not only the cases  $q_0 = 0$  and  $q_0 = 1$  which give the ZAMS and the helium main sequence, but also the cases in between sometimes give insight how stars behave, for instance, in the case where in a close binary system mass flows from one star to its companion. If a primary of, say, one solar mass evolves it forms a helium core, so it resembles a star on a generalized main sequence with a certain value of  $q_0$ . While the evolution goes on  $q_0$  grows while simultaneously the star becomes a red giant. If before the onset of helium burning the surface of it comes close to the companion (to be more precise: when it fills the *Roche lobe*), mass flows from the red giant onto the surface of the still unevolved secondary until only the helium core is left and the original primary after thermal adjustment has become a star of the helium main sequence. In the HR diagram the star has moved from the Red Giant branch to the helium main sequence while its value of  $q_0$  has grown during the mass loss.